

Electron interactions in graphene in a strong magnetic field

M. O. Goerbig,¹ R. Moessner,² and B. Douçot³

¹Laboratoire de Physique des Solides, CNRS UMR 8502, Univ Paris Sud, Orsay, France

²Laboratoire de Physique Théorique de l'École Normale Supérieure, CNRS UMR 8549, Paris, France

³Laboratoire de Physique Théorique et Hautes Energies, CNRS UMR 7589, Univ Paris 6 et 7, Paris, France

(Received 25 April 2006; revised manuscript received 25 September 2006; published 31 October 2006)

Graphene in the quantum Hall regime exhibits a multicomponent structure due to the electronic spin and chirality degrees of freedom. While the applied field breaks the spin symmetry explicitly, we show that the fate of the chirality SU(2) symmetry is more involved: The leading symmetry-breaking terms differ in origin when the Hamiltonian is projected onto the central ($n=0$) rather than any other Landau levels. Our description at the lattice level leads to a Harper equation; in its continuum limit, the ratio of lattice constant a and magnetic length l_B assumes the role of a small control parameter in different guises. The leading symmetry-breaking terms are lattice effects, algebraically small in a/l_B . We analyze the Haldane pseudopotentials for graphene, and evaluate the easy-plane anisotropy of the graphene ferromagnet.

DOI: 10.1103/PhysRevB.74.161407

PACS number(s): 73.43.-f, 71.10.-w, 81.05.Uw

INTRODUCTION

The recent discovery^{1,2} of an integer quantum Hall (QH) effect in a two-dimensional (2D) sheet of graphite, known as graphene, has triggered an avalanche of activity, including on the theory side studies of the transport properties of relativistic Dirac particles,³⁻⁵ the analysis of edge states⁶⁻⁸ and shot noise,⁹ as well as Berry phases in bilayers.¹⁰

In a simple model, electrons in graphene can be treated as hopping on a honeycomb lattice.^{11,12} Perhaps the most salient feature of this problem is the existence in the band structure of a pair of Dirac points with a linear (“relativistic”) energy-momentum relationship. These points are located at the two inequivalent corners of the Brillouin zone (labeled by K and $K'=-K$), endowing graphene with a multicomponent structure analogous to the well-studied examples of bilayer systems, the multivalley structure of silicon, and of course the simple spin degree of freedom. These degrees of freedom can be thought of as SU(2) (or higher symmetry) pseudospins. The resulting Hamiltonian typically contains symmetric terms as well as ones which lower the symmetry, such as Zeeman (spin) or capacitance (bilayer) (Ref. 13) energies.

Here we argue that graphene may be viewed as a further type of multicomponent system. Its internal degree of freedom can be thought of as a chirality:¹⁴ the wave vectors K and K' encode the (anti)clockwise variation of the phase of the electronic wave function on the three sites neighboring any given site on one sublattice.

Moreover, we show that for $n \neq 0$ the chiral SU(2) symmetry is reduced to U(1) in graphene, due to backscattering terms with momentum transfer $2K \sim K$, which provide a coupling of the chirality to the orbital part of the wave function. On the contrary, in $n=0$, the broken symmetry may be due to electrostatic (“Hartree”) effects. Although different in origin, both effects are of order $O(a/l_B)$. The distance between neighboring carbon atoms $a \approx 0.14$ nm provides an additional length scale besides the magnetic length $l_B = \sqrt{\hbar/eB} = 26$ nm/ $\sqrt{B[T]}$, so that $a \ll l_B$. It is somewhat analogous to the layer separation d for bilayers. In graphene for $n \neq 0$, however, only the exchange part of the symmetry-breaking

interaction is nonzero, whereas in bilayers the direct term encodes the capacitance energy, which can be important already for typical values of $d/l_B \sim 1$.

In the following, we flesh out this picture with a microscopic calculation starting at the lattice level, in which we derive and discuss the effective model for interacting electrons restricted to a single relativistic Landau level (LL) and compare it to the nonrelativistic case of electrons in conventional semiconductor heterostructures; the difference between the two is most significant for $n=1$. The backscattering terms are discussed in the case of the QH ferromagnet at the filling factors $\bar{\nu}=1$ of the partially filled LL (for an arbitrary LL, we have $\nu=4n+\bar{\nu}$).

MODEL

The electron field in graphene may be written as a two-spinor whose components, $\psi_\sigma(\mathbf{r}) = \exp(i\sigma\mathbf{K}\cdot\mathbf{r})\chi_\sigma(\mathbf{r})$, are a product of a slowly varying part $\chi_\sigma(\mathbf{r})$ and a rapidly oscillating plane wave with $\sigma\mathbf{K} = \sigma(4\pi/3\sqrt{3}a)\mathbf{e}_x$ for the Brillouin zone corners K and K' (chiralities $\sigma = \pm 1$, respectively). The components of each two-spinor field $\chi_\sigma(\mathbf{r})$ correspond to the two triangular sublattices (labeled by $\alpha = \pm 1$) of the bipartite honeycomb lattice. In a magnetic field with the Landau gauge $\mathbf{A} = (0, Bx)$, q_y is a good quantum number and we may expand $\chi_\alpha(\mathbf{r}) = \exp(iq_y y)g_\alpha(y)$. The electron dynamics (in a tight-binding model with nearest-neighbor hopping $t=1$) is governed by the Harper equation

$$Eg_\alpha^\sigma(x) = -2 \cos \left\{ \sigma \frac{2\pi}{3} + \frac{\sqrt{3}}{2} \left[q_y + \frac{(x + \alpha/4)}{l_B^2} \right] \right\} \times g_{-\alpha}^\sigma \left(x + \frac{\alpha}{2} \right) - g_{-\alpha}^\sigma(x - \alpha), \quad (1)$$

where the distances are measured in units of a . In order to derive a continuum limit in the presence of an unbounded vector potential \mathbf{A} , one expands the cosine in Eq. (1) in the vicinity of x_μ defined as $[q_y + \alpha x_\mu(q_y)/l_B^2]\sqrt{3}/2 = 2\pi\mu$, where μ is an integer which effectively acts as an additional quan-

tum number besides the quasimomentum q_y in the first Brillouin zone.

The continuum limit of Eq. (1) thus reads

$$Eg_\alpha^\sigma(x) = \frac{3}{2} \left(\alpha l_B \partial_x + \sigma \frac{x}{l_B} \right) g_{-\alpha}^\sigma(x),$$

where x is now a small deviation from x_μ . This result coincides with the ones obtained by introducing the minimal coupling $\mathbf{p} \rightarrow \mathbf{p} + e\mathbf{A}$ after deriving the $B=0$ continuum theory.^{14,15} Note that the typical extension of the wave functions along the x axis is $R_L \propto \sqrt{n}l_B$ in the n th LL and the periodicity of x_μ is $\sim l_B^2/a$. The overlap between wave functions with differing μ is therefore exponentially suppressed provided $\sqrt{n} \ll l_B/a$. Finally,

$$\chi_+(\mathbf{r}) = \frac{1}{\sqrt{2}} \sum_{n,m} \begin{pmatrix} i\sqrt{1 + \delta_{n,0}} \langle \mathbf{r} | n, m \rangle \\ \text{sgn}(n) \langle \mathbf{r} | n-1, m \rangle \end{pmatrix} c_{n,m;+}, \quad (2)$$

where the index $+$ represents the K point. In the expression for χ_- (at K'), the components of the spinor are reversed. Here $\text{sgn}(n) = \{1, 0, -1\}$ for $n \{>, =, <\} 0$, respectively. The quantum number n is the index of the relativistic LL, and m is associated with the guiding center operator, which commutes with the one-particle Hamiltonian. The $|n, m\rangle$ are the usual (nonrelativistic) one-particle states for a charged particle in a perpendicular magnetic field. The $c_{n,m;\sigma}$ are fermionic destruction operators.

Projection onto a LL ($n \neq 0$) of the sublattice densities $\rho_\alpha(\mathbf{r}) = \sum_{\sigma,\sigma'} \psi_{\sigma,\alpha}^\dagger(\mathbf{r}) \psi_{\sigma',\alpha}(\mathbf{r})$ gives

$$\rho^n(\mathbf{q}) = \rho_1^n(\mathbf{q}) + \rho_2^n(\mathbf{q}) = \sum_{\sigma,\sigma'} F_n^{\sigma\sigma'}(\mathbf{q}) \bar{\rho}^{\sigma\sigma'}(\mathbf{q}), \quad (3)$$

where the projected density operators read $\bar{\rho}^{\sigma\sigma'}(\mathbf{q}) = \sum_{m,m'} \langle m | \exp\{-i[\mathbf{q} + (\sigma - \sigma')\mathbf{K}] \cdot \mathbf{R}\} | m' \rangle c_{n,m,\sigma}^\dagger c_{n,m',\sigma'}$. The operator \mathbf{R} represents the usual guiding center position, and $\boldsymbol{\eta}$ is the cyclotron coordinate, $\mathbf{r} = \mathbf{R} + \boldsymbol{\eta}$. The chirality-dependent form factors $F_n^{\sigma\sigma'}(\mathbf{q})$ read, in terms of associated Laguerre polynomials $L_n^\alpha(x)$,

$$F_n^{++}(\mathbf{q}) = \frac{1}{2} \left[L_{|n|} \left(\frac{|\mathbf{q}|^2}{2} \right) + L_{|n|-1} \left(\frac{|\mathbf{q}|^2}{2} \right) \right] e^{-|\mathbf{q}|^2/4},$$

$$F_n^{+-}(\mathbf{q}) = \left(\frac{-(q + q^* - K - K^*)}{2\sqrt{2|n|}} \right) L_{|n|-1}^1 \left(\frac{|\mathbf{q} - \mathbf{K}|^2}{2} \right) e^{-|\mathbf{q} - \mathbf{K}|^2/4},$$

where $q = q_x + iq_y$ and $K = K_x + iK_y$ are written in complex notation, and the wave vectors are given in units of $1/l_B$. $F_n^{++}(\mathbf{q}) = F_n^{--}(\mathbf{q})$, and $F_n^{+-}(\mathbf{q})$ is obtained by replacing $\mathbf{q} \rightarrow -\mathbf{q}$ in $F_n^{+-}(\mathbf{q})$.

The Hamiltonian of interacting electrons in graphene, projected onto a single relativistic LL thus reads

$$H = \frac{1}{2} \sum_{\sigma_1, \dots, \sigma_4} \sum_{\mathbf{q}} v_n^{\sigma_1, \dots, \sigma_4}(\mathbf{q}) \bar{\rho}^{\sigma_1 \sigma_3}(-\mathbf{q}) \bar{\rho}^{\sigma_2 \sigma_4}(\mathbf{q}), \quad (4)$$

where the sum over the wave vectors is restricted to the first Brillouin zone. Indeed, the potential consists of a sum over reciprocal lattice vectors, as the local densities [Eq. (3)],

valid for $l_B \gg a$, are restricted to the hexagonal lattice. The chirality-dependent effective interaction

$$v_n^{\sigma_1, \dots, \sigma_4}(\mathbf{q}) = \frac{2\pi e^2}{\epsilon|\mathbf{q}|} F_n^{\sigma_1 \sigma_3}(-\mathbf{q}) F_n^{\sigma_2 \sigma_4}(\mathbf{q}) \quad (5)$$

is not SU(2) symmetric; however, the symmetry-breaking terms are suppressed parametrically in a/l_B . To see this, consider the different form-factor combinations in the effective interaction potential (4).

Terms of the form $F_n^{\sigma,\sigma}(\mp\mathbf{q}) F_n^{\sigma',-\sigma'}(\pm\mathbf{q})$ and ‘‘umklapp scattering’’ terms $[F_n^{\sigma,-\sigma}(-\mathbf{q}) F_n^{\sigma,-\sigma}(\mathbf{q})]$ are exponentially small in a/l_B .

‘‘Backscattering’’ $[F_n^{\sigma,-\sigma}(-\mathbf{q}) F_n^{\sigma,-\sigma}(\mathbf{q})]$: One obtains $v_n^{+-+}(\mathbf{q}) \sim \exp(-|\mathbf{q}|^2/2)/|\mathbf{q}' \pm \mathbf{K}| \sim \exp(-|\mathbf{q}|^2/2)/|\mathbf{K}|$, which is only algebraically small, $v_n^{+-+}/(e^2/\epsilon l_B) \sim a/l_B$, and thus constitutes the leading perturbation to the remaining [SU(2) invariant] terms.

These leading-order terms in the effective interaction yield the SU(2) [or SU(4), if the physical spin is also taken into account] symmetric Hamiltonian (for $n \neq 0$)

$$H_{\text{eff}}^n = \frac{1}{2} \sum_{\sigma,\sigma'} \sum_{\mathbf{q}} \frac{2\pi e^2}{\epsilon|\mathbf{q}|} [\mathcal{F}_n(q)]^2 \bar{\rho}_\sigma(-\mathbf{q}) \bar{\rho}_{\sigma'}(\mathbf{q}), \quad (6)$$

with the graphene form factor

$$\mathcal{F}_n(q) = \frac{1}{2} \left[L_{|n|} \left(\frac{q^2}{2} \right) + L_{|n|-1} \left(\frac{q^2}{2} \right) \right] e^{-q^2/4} \quad (7)$$

and $\bar{\rho}_\sigma(\mathbf{q}) \equiv \bar{\rho}^{\sigma\sigma}(\mathbf{q})$. The graphene form factor (7) has already been written down by Nomura and MacDonald in their study of the QH ferromagnetism at $\bar{\nu}=1$.¹⁶ The leading-order symmetry-breaking correction due to backscattering (BS) is [with $v_n^{\sigma,-\sigma}(\mathbf{q}) \equiv v_n^{\sigma,-\sigma,\sigma,\sigma}(\mathbf{q})]$

$$H_{\text{BS}} = \frac{1}{2} \sum_{\sigma} \sum_{\mathbf{q}} v_n^{\sigma,-\sigma}(\mathbf{q}) \bar{\rho}^{\sigma,-\sigma}(-\mathbf{q}) \bar{\rho}^{-\sigma,\sigma}(\mathbf{q}). \quad (8)$$

The central level ($n=0$) behaves remarkably differently. In this case, the electron chirality σ is equivalent to the sublattice index α [Eq. (2)], and therefore

$$\rho_\alpha^{n=0}(\mathbf{q}) = e^{-q^2/4} \sum_{m,m'} \langle m | e^{-i\mathbf{q} \cdot \mathbf{R}} | m' \rangle c_{n,m;\alpha}^\dagger c_{n,m';\alpha},$$

with the same form factor $\mathcal{F}_{n=0}(q) = e^{-q^2/4}$ as for nonrelativistic electrons in the lowest LL. From an electrostatic point of view, it may be energetically favorable to distribute the electronic density with equal weight on both sublattices. For $n \neq 0$, this follows directly from Eq. (2), but in $n=0$, an equal-weight superposition of $\sigma = \pm 1$ is required to distribute the charges homogeneously on both sublattices. Such an electrostatic effect, compared to the SU(2) invariant terms, is of the same order $O(a/l_B)$ as the backscattering term in $n \neq 0$.

EFFECTIVE INTERACTION

By absorbing the form factor into the interaction, we define

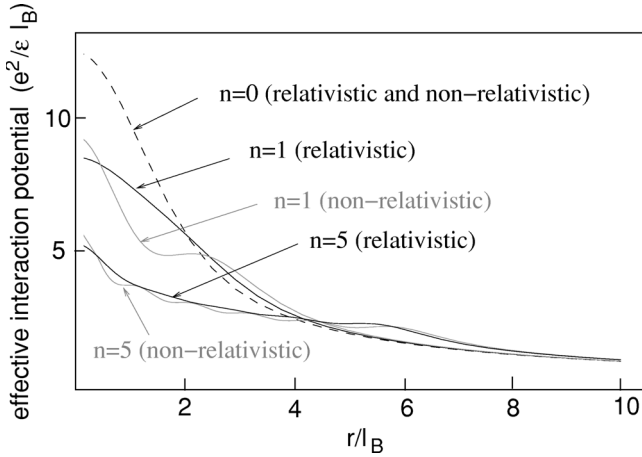


FIG. 1. Effective interaction potentials in real space: Comparison between the relativistic (black lines) and nonrelativistic (gray lines) LLs $n=0, 1$, and 5 . The dashed line represents the interaction potential in $n=0$, which is the same for relativistic and nonrelativistic electrons.

$$v_n(q) = \frac{2\pi e^2}{\epsilon q} [\mathcal{F}_n(q)]^2. \quad (9)$$

Figure 1 shows the effective interaction potentials (9) transformed to real space for $n=0, 1$, and 5 . At large distances, the usual $1/r$ Coulomb potential is obtained. Interestingly, the shape of the interaction potential for the relativistic $n=1$ LL in graphene is more similar to the nonrelativistic $n=0$ level than to the corresponding one $n=1$, as may also be seen in a pseudopotential expansion:¹⁷ $V_\ell^r = (2\pi)^{-1} \sum_{\mathbf{q}} v_n(q) L_\ell(q^2) \exp(-q^2/2)$. Indeed the ratios V_{2m+1}/V_{2m+3} for the odd integer pseudopotentials, which are relevant for the case of polarized electrons, decrease monotonically both in $n=1$ and $n=0$ for relativistic LLs. These ratios, and the differences $V_{2m-1} - V_{2m+1}$, are bigger in the former case, so that—among the polarized states—fractional QH states will therefore be more stable in $n=1$ than in $n=0$ (at constant magnetic field). By contrast, candidate chirality unpolarized states (such as at $\nu=2/3$) fare better for two reasons: First, the fact that the relativistic effective potential is more short-ranged in $n=0$ than in $n=1$ leads to V_0 (and V_0/V_1) being smaller for $n=1$. Secondly, the pair of internal SU(2) degrees of freedom allow for a smaller unpolarized “composite Fermi sphere.”

Numerical results¹⁹ show a first-order phase transition at $V_1/V_3 \approx 1.3$ between the Pfaffian state¹⁸ at $\bar{\nu}=1/2$ and a charge-density wave,²⁰ and a crossover to a composite-fermion Fermi sea when V_1/V_3 is further increased. The Pfaffian state is absent in $n=0$, where $V_1^0/V_3^0=1.6$, probably due to an inaccessible gap.¹⁹ In the relativistic $n=1$ LL, one finds an even larger ratio $V_1^1/V_3^1=1.67$ so that a Pfaffian state is also unlikely to be observed there. Even though the ratio $V_1^2/V_3^2=1.16$ in the relativistic $n=2$ LL is larger than in the corresponding nonrelativistic level ($V_1^2/V_3^2=1.14$), it is well below the critical ratio, and one would thus expect a stripe phase at $\bar{\nu}=1/2$.

It is straightforward to check that the difference to the nonrelativistic case vanishes in the large- n limit (see Fig. 1 for $n=5$), i.e., far from the Dirac points. Replacing $L_n(q^2/2) \exp(-q^2/4) \approx J_0(q\sqrt{2n+1})$, the envelope of $\mathcal{F}_n^2(q) \approx [J_0(q\sqrt{2n-1}) + J_0(q\sqrt{2n+1})]^2/4 \approx J_0^2(q\sqrt{2n})$ agrees to leading order in $1/n$ with the nonrelativistic case.

QH FERROMAGNET AT $\bar{\nu}=1$

In recent transport measurements on a single graphene sheet additional integer QH plateaus beyond those corresponding to $\nu=4n$ have been observed.²¹ These appear as the first signature of electron-electron interactions, and the analogy with the nonrelativistic case in semiconductor heterostructures hints at a chirality QH ferromagnet. The stability of such a state, in the presence of impurities, has been investigated by Nomura and MacDonald.¹⁶ We now analyze the impact of the backscattering term (8) on such a ferromagnet for $n \neq 0$, within the Hartree-Fock (HF) approximation. Following Ref. 13, we consider the HF trial state $|\Psi\rangle = \Pi_m (u_m c_{m,+}^\dagger + v_m c_{m,-}^\dagger) |0\rangle$, where we may parametrize $u_m = \cos(\theta_m/2) e^{-i\phi_m/2}$ and $v_m = \sin(\theta_m/2) e^{i\phi_m/2}$, in terms of the real angle fields θ_m and ϕ_m , which can be thought of as polar coordinates of a vector field $\mathbf{n}(m)$. In the case of a SU(2)-symmetric repulsive interaction, it has been shown that the trial state $|\Psi\rangle$ minimizes the energy for constant θ_m and ϕ_m , thus yielding a simple ferromagnet.¹³ The backscattering term, averaged over this state, is, apart from an unimportant constant C ,

$$\langle H_{\text{BS}} \rangle = \frac{1}{4} \sum_{m,m'} \{ V_{m,m',m,m'}^{\text{BS}} [n_x(m)n_x(m') + x \rightarrow y] + V_{m,m',m',m}^{\text{BS}} n_z(m)n_z(m') \} + C, \quad (10)$$

$$V_{m_1 \dots m_4}^{\text{BS}} \approx \frac{\pi e^2}{\epsilon |\mathbf{K}|} \sum_{\mathbf{q}} \frac{|\mathbf{q}|^2}{2|n|} \left[L_{|n|-1}^1 \left(\frac{|\mathbf{q}|^2}{2} \right) e^{-|\mathbf{q}|^2/4} \right]^2 \times \langle m_1 | e^{i\mathbf{q}\cdot\mathbf{R}} | m_3 \rangle \langle m_2 | e^{-i\mathbf{q}\cdot\mathbf{R}} | m_4 \rangle. \quad (11)$$

The factor of $|\mathbf{q}|^2$ in this sum is due to the fact that the wave functions on the same sublattice, but for different chiralities, are orthogonal. A gradient expansion¹³ yields to lowest order an easy-plane anisotropy Δ_z :

$$\langle H_{\text{BS}} \rangle^{(0)} = \sum_m \Delta_z [n_z(m)]^2, \quad \Delta_z = \frac{1}{16\pi^2} \frac{e^2}{\epsilon |\mathbf{K}|}. \quad (12)$$

This is reminiscent of the bilayer case, where a finite layer separation also induces easy-plane ferromagnetism. The key differences are the following. (i) The parameter $a/l_B \sim 10^{-2}$, which mimicks the “layer separation,” is tiny for currently experimentally accessible magnetic fields. This implies a Curie temperature $\Theta \sim e^2/k_B \epsilon l_B$, whereas the crossover to easy-plane behavior does not become visible until a logarithmically (in a/l_B) small energy. As chirality ferromagnetism involves neither electric nor magnetic dipole ordering, inter-plane coupling in a multilayer system will be suppressed. This opens the perspective of probing the 2D behavior for

instance in specific-heat measurements. (ii) Contrary to the bilayer case and the relativistic $n=0$ LL, the gap is not due to a charging energy when only one layer is filled—there is no contribution to Eq. (12) from the direct interaction because $v_n^\pm(q=0)=0$ [Eq. (5)]. (iii) Δ_z is a lattice effect—it vanishes linearly in a as the lattice constant tends to zero at fixed l_B . It does not depend on n , whereas the SU(2) symmetric terms scale as $e^2/\epsilon\sqrt{n}$ in the large- n limit. Note, however, that the continuum limit based on the Dirac equation ceases to be valid when $R_L \sim \sqrt{nl_B} \sim l_B^2/a$.

COMPARISON WITH EXPERIMENT

Zhang *et al.* have observed additional Hall plateaus corresponding to $\nu=0, \pm 1$ ($n=0$), and $\nu=\pm 4$ ($n=1$).²¹ The former pair corresponds to a complete resolution of the four-fold degeneracy of LLs corresponding to different internal (spin and chirality) degrees of freedom in $n=0$. An explanation of this has to consider the size of the disorder broadening of the LLs, Γ , compared to their splitting due to the cost of exciting quasiparticles away from integer filling.¹⁶ An experimental estimate yields $\Gamma \sim 1.7$ meV.²¹

Using our above results, we find that these quasiparticles are Skyrmions for $n=0, 1$, whose energy cost $E_{SK}=4\pi\rho_s$ is obtained within the nonlinear sigma model,¹³ with the help of the stiffness

$$\rho_s = \frac{1}{32\pi^2} \int_0^\infty dq q^3 v_n(q).$$

One obtains for the experimentally relevant parameters (at 17 T with dielectric constant²² $\epsilon \sim 5$) $E_{SK}=4\pi\rho_s = 7/64\sqrt{\pi/2}e^2/\epsilon l_B \sim 1.8$ meV ($n=1$) and, for $n=0$, $E_{SK} = 1/4\sqrt{\pi/2}e^2/\epsilon l_B \sim 4$ meV, both for SU(2) or SU(4).²³ In addition, there is a contribution from anisotropies, mainly the Zeeman effect (about $E_Z=0.1B[T]$ meV); the chirality-

symmetry breaking due to lattice effects, being of order ~ 0.05 meV, plays only a minor role here.

The activation gap at $\nu=\pm 4$ scales linearly with B , indicating a relevant Zeeman effect, and the plateau is visible from ~ 17 T onward.²¹ Given the Skyrmions in $n=0$ are more costly than the sum of E_{SK} and E_Z in $n=1$, this explains why the chirality Landau levels are resolved at 17 T in $n=0$, even without the help of an anisotropy field, whereas they remain absent at $\nu=\pm 3, \pm 5$ in fields up to 45 T. In fact, for $n=1$, E_{SK} does not reach 4 meV for fields below 80 T; also the plateau at $\nu=0$ disappears below 11 T, where $E_{SK} \sim 3$ meV.

To summarize, we have analyzed a microscopic model for interaction effects in graphene in the QH regime. We find corrections to the SU(2) chirality-symmetric model to be numerically much smaller than the Zeeman energy breaking the SU(2) spin-symmetry. In addition, the effective interaction potential differs from the nonrelativistic case most strongly for small but nonzero n , in particular $n=1$, which will therefore be a good place to look for interaction physics different from the GaAs heterostructure. Finally, recent experiments suggest the presence of chirality ferromagnetism and Skyrmions in graphene.

Note added. Recently, QH articles of related work have appeared by Alicea and Fisher²⁴ on ferromagnetism at the integer effect and by Apalkov and Chakraborty²⁵ on exact diagonalizations in the fractional QH regime using the above-mentioned pseudopotentials.

ACKNOWLEDGMENTS

We thank N. Cooper, J.-N. Fuchs, D. Huse, P. Lederer, and S. Sondhi for fruitful discussions. M.O.G. is grateful for a stimulating interaction in the LPS' "Journal Club Mesoscopic Physics."

¹K. S. Novoselov, A. K. Geim, S. V. Morosov, D. Jiang, M. I. Katsnelson, I. V. Grigorieva, S. V. Dubonos, and A. A. Firsov, *Nature (London)* **438**, 197 (2005).

²Y. Zhang, Y.-W. Tan, H. L. Stormer, and P. Kim, *Nature (London)* **438**, 201 (2005).

³V. P. Gusynin and S. G. Sharapov, *Phys. Rev. Lett.* **95**, 146801 (2005); *Phys. Rev. B* **73**, 245411 (2006).

⁴M. I. Katsnelson, *Eur. Phys. J. B* **51**, 157 (2006).

⁵N. M. R. Peres, F. Guinea, and A. H. Castro Neto, *Phys. Rev. B* **73**, 125411 (2006).

⁶A. H. Castro Neto, F. Guinea, and N. M. R. Peres, *Phys. Rev. B* **73**, 205408 (2006).

⁷L. Brey and H. A. Fertig, *Phys. Rev. B* **73**, 195408 (2006).

⁸D. A. Abanin, P. A. Lee, and L. S. Levitov, *Phys. Rev. Lett.* **96**, 176803 (2006).

⁹J. Tworzydło, B. Trauzettel, M. Titov, A. Rycerz, and C. W. J. Beenakker, *Phys. Rev. Lett.* **96**, 246802 (2006).

¹⁰E. McCann and V. I. Fal'ko, *Phys. Rev. Lett.* **96**, 086805 (2006).

¹¹P. R. Wallace, *Phys. Rev.* **71**, 622 (1947).

¹²J. C. Slonczewski and P. R. Weiss, *Phys. Rev.* **109**, 272 (1958).

¹³K. Moon, H. Mori, K. Yang, S. M. Girvin, A. H. MacDonald, L. Zheng, D. Yoshioka, and S.-C. Zhang, *Phys. Rev. B* **51**, 5138

(1995).

¹⁴F. D. M. Haldane, *Phys. Rev. Lett.* **61**, 2015 (1988).

¹⁵Y. Zheng and T. Ando, *Phys. Rev. B* **65**, 245420 (2002).

¹⁶K. Nomura and A. H. MacDonald, *Phys. Rev. Lett.* **96**, 256602 (2006).

¹⁷F. D. M. Haldane, *Phys. Rev. Lett.* **51**, 605 (1983).

¹⁸G. Moore and N. Read, *Nucl. Phys. B* **360**, 362 (1991).

¹⁹E. H. Rezayi and F. D. M. Haldane, *Phys. Rev. Lett.* **84**, 4685 (2000).

²⁰A. A. Koulakov, M. M. Fogler, and B. I. Shklovskii, *Phys. Rev. Lett.* **76**, 499 (1996); R. Moessner and J. T. Chalker, *Phys. Rev. B* **54**, 5006 (1996).

²¹Y. Zhang, Z. Jiang, J. P. Small, M. S. Purewal, Y.-W. Tan, M. Fazlollahi, J. D. Chudow, J. A. Jaszczak, H. L. Stormer, and P. Kim, *Phys. Rev. Lett.* **96**, 136806 (2006).

²²J. González, F. Guinea, and M. A. H. Vozmediano, *Phys. Rev. B* **59**, R2474 (1999).

²³D. P. Arovas, A. Karlhede, and D. Lilliehook, *Phys. Rev. B* **59**, 13147 (1999).

²⁴J. Alicea and M. P. A. Fisher, *Phys. Rev. B* **74**, 075422 (2006).

²⁵V. M. Apalkov and T. Chakraborty, *Phys. Rev. Lett.* **97**, 126801 (2006).